FEC Recovery Performance for Video Streaming Services over Wired-Wireless Networks

Shun Muraoka [a], Hiroyuki Masuyama [a], Shoji Kasahara [a,*],
Yutaka Takahashi [a],

[a]*Graduate School of Informatics, Kyoto University*
Yoshida-honmachi, Sakyo-ku, Kyoto 606-8501, Japan

Abstract

This paper considers the packet recovery performance of forward error correction (FEC) for video streaming services over wired-wireless networks. Focusing on a wireless base station, we model it as a single-server queueing system with a Markovian service process in which the state of the server alternates between Good and Bad states. The system has two independent input processes: one is a general renewal input process and the other is a Poisson arrival process. We analyze the packet- and block-level loss probabilities to investigate the recovery performance of FEC at block level. The analysis is validated with simulation experiments driven by real traffic traces. Numerical examples show that the block-loss probability is greatly affected by the system capacity and the mean Bad-state period, and that the recovery performance of FEC deteriorates according to the fluctuation in the packet transmission rate at a wireless base station.

Key words: Single-server queue with two input processes, Markovian service process, forward error correction, general renewal input, block-loss probability.

1 Introduction

Recent advancement of video coding techniques and wide spread of broadband networks accelerate the development of real-time applications such as video streaming, sports live broadcasting and web conference. With the rapid growth of wireless networks, these applications are expected to be widely deployed over wireless networks. Because video applications have stringent delay constraint, many techniques

---

* Corresponding author. Tel: +81-75-753-5493; Fax: +81-75-753-3358.
  Email address: `kasahara@ieee.org` (Shoji Kasahara).

have been studied to guarantee video image quality over wireless networks where burst packet loss occurs due to mobility and interference.

There are two basic techniques for packet-loss recovery: Automatic Repeat reQuest (ARQ) and Forward Error Correction (FEC). ARQ is a typical acknowledgement-based error recovery technique. In ARQ, lost data packets are retransmitted by the sender host. However, this retransmission mechanism is activated by receiving duplicate acknowledgement (ACK) packets or timer time-out, causing a large end-to-end delay. This large delay is not suitable for real-time applications such as video streaming and web conference.

On the other hand, FEC is a well-known coding-based error recovery scheme [3,16]. In FEC, redundant data is generated from original data, and a sender host transmits both the original and redundant data to a receiver host. When some part of the original data is lost, it can be recovered from the redundant data at the receiver host if the loss is below a prespecified level. In this paper, we focus on packet-level FEC scheme [17]. When N redundant data packets are generated from D original data packets, the lost data can be recovered completely if the number of lost packets is less than or equal to N. Because FEC requires no retransmission mechanism, it is a suitable packet-loss recovery scheme for video applications with stringent delay constraint.

With the recent development of optical networking technology such as wavelength division multiplexing (WDM), the bottleneck of data transmission shifts from backbone networks to access ones (the last mile bandwidth bottleneck [12]). On the other hand, wireless mesh networks (WMNs) have attracted considerable attention as a solution of the last mile issue for access networks [1]. WMNs consist of wireless mesh routers and mesh clients, and are expected to support a variety of applications to end users.

Now consider video streaming services over the wired-wireless network consisting of optical backbone networks and wireless access networks. Here, video streaming servers are placed on the backbone networks, while a client node is connected to a wireless base station with one-hop wireless link. In this situation, the wireless base station is likely to be the bottleneck of data transmission for video streaming service due to interference and user mobility. The quality of service (QoS) of video streaming over the wired-wireless network is significantly affected by the packet loss process at the wireless base station. Note that data packets for video streaming are sent to the client node at a constant bit rate. Because the optical backbone networks provide a high-speed transmission, it is important to consider the case where inter-arrival times of packets to the edge wireless base station are almost the same.

In this paper, focusing on the wireless base station, we consider the packet recovery performance of FEC at the wireless base station. We consider a single-server queue-

ing system with finite buffer, in which the service time of a customer is governed by a two-state Markovian service process. The system has two inputs: main traffic and background traffic. Main traffic consists of original packets and FEC redundant ones. We assume that the inter-arrival times of packets in main traffic are independent and identically distributed (i.i.d.) according to a general distribution. On the other hand, arriving packets in background traffic form a Poisson process. Note that the assumption of main traffic enables us to describe various arrival processes including constant inter-arrival times. We analyze the packet- and block-level loss probabilities of main traffic, evaluating the recovery performance of FEC.

The rest of this paper is organized as follows. Section 2 gives an overview of the previous studies on the performance analysis of FEC recovery. Section 3 describes our analytical model, and Section 4 derives performance measures. Numerical examples are presented in Section 5, and finally Section 6 provides some conclusions.

2 Related work

It is well known that the recovery performance of FEC is significantly affected by the packet loss process, and much effort has been devoted to the development of adaptive QoS control schemes to improve the video quality [6,7,10,11]. The relation between the recovery performance and the redundancy of FEC has also been extensively studied in the literature. A pioneering work is [5] in which the distribution of the number of lost packets within a block of packets is analyzed for an M/M/1/K queue with first-in first-out (FIFO) discipline. Altman and Jean-Marie [2] considered the loss probability of a block of packets, investigating the effect of FEC redundancy on the block-loss probability. Note that the above works assumed a single Poissonian source.

In terms of the generalization of the packet arrival process, Kawahara et al. [14] considered a discrete-time finite-buffer queuing model with two arrival processes, evaluating the recovery capability of FEC. In [14], main packet traffic consisting of original and redundant packets is modeled as an interrupted Bernoulli process, and background traffic is assumed as a Markov modulated Bernoulli process. Hellal et al. [13] considered an M/M/1/K queue in which packets arrive at the system from several independent sources, and analyzed the distribution of the number of lost packets within a block of packets. In [13], they also extended the model to the one where the sequences of service times and inter-arrival times of packets are ergodic and the system capacity is equal to one, discussing the qualitative nature of redundancy scheme. In [18], a technique combining priority-based cell discarding and FEC was proposed for guaranteeing the video QoS over asynchronous transfer mode (ATM) networks. The performance of the basic hybrid block-loss reduction scheme was analyzed with an M/M/1/K queue in which cells from sessions using FEC are multiplexed with cells from sessions without FEC, and several buffer-

management policies were thoroughly investigated by simulation.

Dán et al. [8,9] considered the effect of the packet size distribution (PSD) on the packet loss process in finite queueing systems with two input processes. In [8], they considered the system with two input processes: one is a Markov-modulated Poisson process (MMPP) and the other is a Poisson one. The FEC performance was numerically evaluated for deterministic and exponential PSDs. In [9], the loss process of an MMPP+MMPP/E_r/1/K queue was analyzed. The analysis was validated by simulation experiments driven by traces measured in a backbone network for the Internet. It was claimed that the PSD for evaluating FEC performance over the current Internet can be well approximated by the exponential distribution.

In [15], focusing on the bottleneck edge router, we considered the packet recovery performance of FEC for a single-server queueing system with finite buffer fed by two input processes: one is a general renewal input process, and the other is Poisson arrival process. Assuming that the PSD is exponential, we analyzed the packet- and block-level loss probabilities. It was found that the block-loss probability is significantly improved by FEC when the system accommodates a small number of packets. In this paper, focusing on the wireless base station, we extend the model in [15] for investigating the recovery performance of FEC over wired-wireless networks.

3   GI+M/MSP/1/K queueing model

We consider the transmission of a data block consisting of D packets. Suppose N redundant packets are generated from the original D packets, and a set of M packets are transmitted as main traffic, where $M = D + N$. We assume that a packet loss occurs only at the wireless base station. We also assume that if the number of lost packets among the M packets is less than or equal to N, the original data block can be retrieved at the destination by FEC decoding and otherwise cannot be retrieved, resulting in a block loss.

We model the wireless base station as a FIFO single-server queueing system with a buffer of capacity $K - 1$. Thus the total capacity of the system is equal to K. The inter-arrival times of packets in main traffic are i.i.d with a general distribution $G(x)$. Background traffic is also multiplexed with main traffic at the system, and we assume that packet arrivals in background traffic form a Poisson process with rate λ. For the packet transfer process over the wireless link, we consider a Markovian service process with two states "Good" and "Bad", which was developed originally in [4] for a wireless channel model. In the following, "Good" and "Bad" are denoted by "G" and "B", respectively. The lengths of G and B states are i.i.d. according to exponential distributions with parameters α and β, respectively. While being in state G (resp. B), the departure rate of packets is equal to μ_G (resp. μ_B), where

$\mu_G > \mu_B$.

In what follows, we call the queueing system GI+M/MSP/1/K.

4 Derivation of performance measures

In this section, we first consider the packet-loss probability of main traffic. We then derive the block-loss probability of a block, which consists of D original data packets and N redundant packets.

4.1 Packet-loss probability of main traffic

Let $L(t)$ ($t \geq 0$) denote the number of packets in the system at time t. Let $S(t)$ ($t \geq 0$) denote the state of the server at time t. We assume that $L(t)$ and $S(t)$ are right-continuous and have left-hand limits, respectively. Let $\widehat{T}_\nu$ ($\nu = 1, 2, \dots$) denote the arrival epoch of the νth packet in main traffic at the system. We assume $\widehat{T}_1 = 0$ hereafter. We then have

$$L(\widehat{T}_\nu) = \min(L(\widehat{T}_\nu-) + 1, K), \qquad \nu = 1, 2, \dots, \tag{1}$$

$$S(\widehat{T}_\nu) = S(\widehat{T}_\nu-), \qquad \nu = 1, 2, \dots. \tag{2}$$

Let $\boldsymbol{\pi}_l(t) = (\pi_{l,G}(t), \pi_{l,B}(t))$ ($l = 0, 1, \dots, K$), where $\pi_{l,s}(t) = \Pr[L(t) = l, S(t) = s]$ for $s = G, B$. From (1) and (2), we have

$$\boldsymbol{\pi}_0(\widehat{T}_\nu) = \mathbf{0}, \tag{3}$$

$$\boldsymbol{\pi}_l(\widehat{T}_\nu) = \boldsymbol{\pi}_{l-1}(\widehat{T}_\nu-), \qquad l = 1, 2, \dots, K-1, \tag{4}$$

$$\boldsymbol{\pi}_K(\widehat{T}_\nu) = \boldsymbol{\pi}_{K-1}(\widehat{T}_\nu-) + \boldsymbol{\pi}_K(\widehat{T}_\nu-). \tag{5}$$

Let $\boldsymbol{\pi}(t) = (\boldsymbol{\pi}_0(t), \boldsymbol{\pi}_1(t), \dots, \boldsymbol{\pi}_K(t))$. Let $\boldsymbol{\Lambda}$ denote a $2(K+1) \times 2(K+1)$ matrix such that

$$\boldsymbol{\Lambda} = \begin{pmatrix} \boldsymbol{O} & \boldsymbol{I}_2 & \boldsymbol{O} & \dots & \boldsymbol{O} & \boldsymbol{O} \\ \boldsymbol{O} & \boldsymbol{O} & \boldsymbol{I}_2 & \ddots & \boldsymbol{O} & \boldsymbol{O} \\ \vdots & \vdots & \ddots & \ddots & \vdots & \vdots \\ \boldsymbol{O} & \boldsymbol{O} & \boldsymbol{O} & \ddots & \boldsymbol{I}_2 & \boldsymbol{O} \\ \boldsymbol{O} & \boldsymbol{O} & \boldsymbol{O} & \dots & \boldsymbol{O} & \boldsymbol{I}_2 \\ \boldsymbol{O} & \boldsymbol{O} & \boldsymbol{O} & \dots & \boldsymbol{O} & \boldsymbol{I}_2 \end{pmatrix},$$
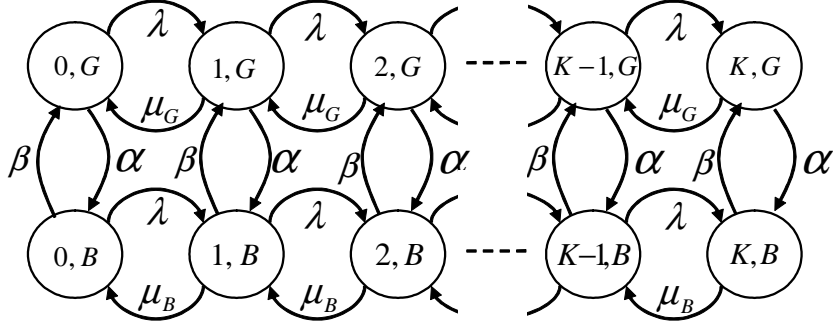
Fig. 1. State transition diagram of $(L(t), S(t))$.

where $\boldsymbol{I}_2$ is a 2×2 identity matrix. It then follows from (3), (4) and (5) that

$$\boldsymbol{\pi}(\widehat{T}_\nu) = \boldsymbol{\pi}(\widehat{T}_\nu-)\boldsymbol{\Lambda}, \qquad \nu = 1, 2, \ldots. \tag{6}$$

Recall here that during time interval $(\widehat{T}_\nu, \widehat{T}_{\nu+1})$, there are no arrivals from main traffic and packets from background traffic arrive at the system according to a Poisson process with rate λ. Recall also that the service process is Markovian. Thus during time interval $(\widehat{T}_\nu, \widehat{T}_{\nu+1})$, $\{(L(t), S(t)); t \geq 0\}$ is a continuous-time bivariate Markov chain (see Fig. 1).

Arranging the states of the bivariate Markov chain in lexicographical order, its generator $\boldsymbol{Q}$ is of size $2(K+1) \times 2(K+1)$ and is given by

$$\boldsymbol{Q} = \begin{pmatrix} \boldsymbol{A}_1 & \lambda\boldsymbol{I}_2 & \boldsymbol{O} & \ldots & \boldsymbol{O} & \boldsymbol{O} \\ \boldsymbol{B} & \boldsymbol{A}_2 & \lambda\boldsymbol{I}_2 & \ddots & \vdots & \vdots \\ \boldsymbol{O} & \boldsymbol{B} & \boldsymbol{A}_2 & \ddots & \boldsymbol{O} & \boldsymbol{O} \\ \boldsymbol{O} & \boldsymbol{O} & \boldsymbol{B} & \ddots & \lambda\boldsymbol{I}_2 & \boldsymbol{O} \\ \vdots & \vdots & \ddots & \ddots & \boldsymbol{A}_2 & \lambda\boldsymbol{I}_2 \\ \boldsymbol{O} & \boldsymbol{O} & \boldsymbol{O} & \ddots & \boldsymbol{B} & \boldsymbol{A}_3 \end{pmatrix},$$

where

$$\boldsymbol{A}_1 = \begin{pmatrix} -(\alpha + \lambda) & \alpha \\ \beta & -(\beta + \lambda) \end{pmatrix}, \qquad \boldsymbol{A}_2 = \begin{pmatrix} -(\alpha + \lambda + \mu_G) & \alpha \\ \beta & -(\beta + \lambda + \mu_B) \end{pmatrix},$$

$$\boldsymbol{A}_3 = \begin{pmatrix} -(\alpha + \mu_G) & \alpha \\ \beta & -(\beta + \mu_B) \end{pmatrix}, \quad \boldsymbol{B} = \begin{pmatrix} \mu_G & 0 \\ 0 & \mu_B \end{pmatrix}.$$

6

Because inter-arrival times of main traffic are i.i.d. with distribution $G(x)$, we have

$$\boldsymbol{\pi}(\widehat{T}_{\nu+1}-) = \boldsymbol{\pi}(\widehat{T}_\nu)\boldsymbol{\Gamma}, \qquad \nu = 1, 2, \ldots, \tag{7}$$

where

$$\boldsymbol{\Gamma} = \int_0^\infty \exp(\boldsymbol{Q}x) dG(x).$$

It follows from (6) and (7) that

$$\boldsymbol{\pi}(\widehat{T}_{\nu+1}-) = \boldsymbol{\pi}(\widehat{T}_\nu-)\boldsymbol{\Lambda}\boldsymbol{\Gamma}, \qquad \nu = 1, 2, \ldots. \tag{8}$$

Let T_m ($m = 1, 2, \ldots$) denote $\widehat{T}_{\nu+m}$. In what follows, setting $\nu \to \infty$, we assume that the system already reaches the steady state at time T_1. For simplicity, we denote $\boldsymbol{\pi}_l(T_1-)$ and $\boldsymbol{\pi}(T_1-)$ by $\boldsymbol{\pi}_l^-$ and $\boldsymbol{\pi}^-$, respectively. It follows from (8) that

$$\boldsymbol{\pi}^- = \boldsymbol{\pi}^-\boldsymbol{\Lambda}\boldsymbol{\Gamma}, \qquad \boldsymbol{\pi}^-\boldsymbol{e} = 1,$$

where $\boldsymbol{e}$ denotes a column vector of ones with an appropriate dimension. Let P_{loss} denote the packet-loss probability of main traffic. Note here that a packet in main traffic is lost only when the queue length on arrival is equal to K. We then have

$$P_{loss} = \boldsymbol{\pi}_K^-\boldsymbol{e}.$$

4.2   Block-loss probability

This subsection derives the block-loss probability $P_{loss}^{(B)}$, which is defined as the probability that the FEC decoding fails to retrieve data packets of a block, i.e., the number of lost packets among M packets of a block is greater than that of the redundant packets, N. We focus on an arbitrary block and call it tagged block hereafter. We assume that the M packets of the tagged block arrive continuously to the system at time T_1 through T_M. We then call the packet arriving at time T_m ($m = 1, 2, \ldots, M$) packet m. We define L_m^- and L_m ($m = 1, 2, \ldots, M$) as the number of packets in the system at time T_m- and T_m, respectively, i.e., $L_m^- = L(T_m-)$ and $L_m = L(T_m)$. We also define S_m^- and S_m ($m = 1, 2, \ldots, M$) as the states of the server at time T_m- and T_m, respectively. Let N_m ($m = 1, 2, \ldots, M$) denote the number of lost packets among packet 1 through m. Let $\boldsymbol{p}(m, k) = (\boldsymbol{p}_1(m, k), \boldsymbol{p}_2(m, k), \ldots, \boldsymbol{p}_K(m, k))$ ($m = 0, 1, \ldots, M$, $k = 0, 1, \ldots, M$), where $\boldsymbol{p}_l(m, k)$ ($l = 1, 2, \ldots, K$) denotes a 1×2 vector such that

$$\boldsymbol{p}_l(m, k) = (\Pr[N_m = k, L_m = l, S_m = G], \ \Pr[N_m = k, L_m = l, S_m = B]).$$

The block-loss probability $P_{loss}^{(B)}$ is then given by

$$P_{loss}^{(B)} = \Pr[N_M > N] = 1 - \sum_{k=0}^N \boldsymbol{p}(M, k)\boldsymbol{e}.$$

In the rest of this subsection, we establish the recursion for the $\boldsymbol{p}(m,k)$. We first derive $\boldsymbol{p}(1,k)$. If $L_1^- < K$, packet 1 can enter the system and therefore $L_1 = L_1^- + 1$. Note that $S_1 = S_1^-$. Thus $\boldsymbol{p}_l(1,0)$ $(l = 1, 2, \ldots, K)$ is given by

$$
\begin{aligned}
\boldsymbol{p}_l(1,0) &= (\Pr[L_1 = l, S_1 = G], \Pr[L_1 = l, S_1 = B]) \\
&= (\Pr[L_1^- = l - 1, S_1^- = G], \Pr[L_1^- = l - 1, S_1^- = B]) \\
&= \boldsymbol{\pi}_{l-1}^-.
\end{aligned}
\tag{9}
$$

On the other hand, if $L_1^- = K$, packet 1 is lost and $L_1 = K$. Therefore we have

$$
\boldsymbol{p}_l(1,1) = \begin{cases} \mathbf{0}, & l = 1, 2, \ldots, K-1, \\ \boldsymbol{\pi}_K^-, & l = K. \end{cases}
\tag{10}
$$

Because $N_1 \leq 1$, we obtain

$$
\boldsymbol{p}_l(1,k) = \mathbf{0}, \qquad \forall k = 2, 3, \ldots, M, \ \forall l = 1, 2, \ldots, K.
\tag{11}
$$

From (9), (10) and (11), we have

$$
\boldsymbol{p}(1,k) = \begin{cases} (\boldsymbol{\pi}_0^-, \boldsymbol{\pi}_1^-, \ldots, \boldsymbol{\pi}_{K-1}^-), & k = 0, \\ (\mathbf{0}, \mathbf{0}, \ldots, \mathbf{0}, \boldsymbol{\pi}_K^-), & k = 1, \\ \mathbf{0}, & k = 2, 3, \ldots, M. \end{cases}
\tag{12}
$$

Next, we derive $\boldsymbol{p}(m,k)$ for $m = 2, 3, \ldots, M$. Let $\boldsymbol{A}_{i,j}(\sigma)$ $(i, j = 1, 2, \ldots, K)$ denote a 2×2 matrix such that

$$
\boldsymbol{A}_{i,j}(\sigma) = \begin{pmatrix} \Pr[(j,G)_m, \Theta_m = \sigma \mid (i,G)_{m-1}] & \Pr[(j,B)_m, \Theta_m = \sigma \mid (i,G)_{m-1}] \\ \Pr[(j,G)_m, \Theta_m = \sigma \mid (i,B)_{m-1}] & \Pr[(j,B)_m, \Theta_m = \sigma \mid (i,B)_{m-1}] \end{pmatrix},
$$

where $(l,s)_m$ denotes event $\{L_m = l, S_m = s\}$, and where $\Theta_m = 1$ if packet m is lost, and otherwise $\Theta_m = 0$. We then define $\boldsymbol{A}(\sigma)$ $(\sigma = 0, 1)$ as

$$
\boldsymbol{A}(\sigma) = \begin{pmatrix} \boldsymbol{A}_{1,1}(\sigma) & \boldsymbol{A}_{1,2}(\sigma) & \cdots & \boldsymbol{A}_{1,K}(\sigma) \\ \boldsymbol{A}_{2,1}(\sigma) & \boldsymbol{A}_{2,2}(\sigma) & \cdots & \boldsymbol{A}_{2,K}(\sigma) \\ \vdots & \vdots & \ddots & \vdots \\ \boldsymbol{A}_{K,1}(\sigma) & \boldsymbol{A}_{K,2}(\sigma) & \cdots & \boldsymbol{A}_{K,K}(\sigma) \end{pmatrix}.
$$

8

It is easy to see that for $m = 2, 3, \ldots, M$, $N_m \leq m$ and therefore

$$
\boldsymbol{p}(m, k) = \begin{cases} \boldsymbol{p}(m-1, 0)\boldsymbol{A}(0), & k = 0, \\ \boldsymbol{p}(m-1, k-1)\boldsymbol{A}(1) + \boldsymbol{p}(m-1, k)\boldsymbol{A}(0), & k = 1, 2, \ldots, m, \\ \boldsymbol{0}, & k = m+1, m+2, \ldots, M, \end{cases}
$$

from which and (12) we can compute $\boldsymbol{p}(m, k)$'s.

Finally we close this subsection by deriving $\boldsymbol{A}(\sigma)$ ($\sigma = 0, 1$). Let $\boldsymbol{\Gamma}_{i,j}$ ($i = 0, 1, \ldots, K$, $j = 0, 1, \ldots, K$) denote a 2×2 matrix such that

$$
\boldsymbol{\Gamma} = \begin{pmatrix} \boldsymbol{\Gamma}_{0,0} & \boldsymbol{\Gamma}_{0,1} & \cdots & \boldsymbol{\Gamma}_{0,K} \\ \boldsymbol{\Gamma}_{1,0} & \boldsymbol{\Gamma}_{1,1} & \cdots & \boldsymbol{\Gamma}_{1,K} \\ \vdots & \vdots & \ddots & \vdots \\ \boldsymbol{\Gamma}_{K,0} & \boldsymbol{\Gamma}_{K,1} & \cdots & \boldsymbol{\Gamma}_{K,K} \end{pmatrix}.
$$

Note that if $L_m^- < K$, $\Theta_m = 0$, $L_m = L_m^- + 1$ and $S_m = S_m^-$. We then have

$$
\begin{aligned}
\boldsymbol{A}_{i,j}(0) &= \begin{pmatrix} \Pr[(j-1, G)_m^- \mid (i, G)_{m-1}] & \Pr[(j-1, B)_m^- \mid (i, G)_{m-1}] \\ \Pr[(j-1, G)_m^- \mid (i, B)_{m-1}] & \Pr[(j-1, B)_m^- \mid (i, B)_{m-1}] \end{pmatrix} \\
&= \boldsymbol{\Gamma}_{i, j-1},
\end{aligned} \tag{13}
$$

where $(l, s)_m^-$ denotes event $\{L_m^- = l, S_m^- = s\}$. Further because $\{\Theta_m = 1\}$ is equivalent to $\{L_m = L_m^- = K\}$, we have

$$
\boldsymbol{A}_{i,j}(1) = \begin{cases} \boldsymbol{O}, & j = 1, 2, \ldots, K-1, \\ \boldsymbol{\Gamma}_{i,K}, & j = K. \end{cases} \tag{14}
$$

It follows from (13) and (14) that

9

$$
\boldsymbol{A}(0) = \begin{pmatrix} \boldsymbol{\Gamma}_{1,0} & \boldsymbol{\Gamma}_{1,1} & \cdots & \boldsymbol{\Gamma}_{1,K-1} \\ \boldsymbol{\Gamma}_{2,0} & \boldsymbol{\Gamma}_{2,1} & \cdots & \boldsymbol{\Gamma}_{2,K-1} \\ \vdots & \vdots & \ddots & \vdots \\ \boldsymbol{\Gamma}_{K,0} & \boldsymbol{\Gamma}_{K,1} & \cdots & \boldsymbol{\Gamma}_{K,K-1} \end{pmatrix},
$$

$$
\boldsymbol{A}(1) = \begin{pmatrix} \boldsymbol{O} & \cdots & \boldsymbol{O} & \boldsymbol{\Gamma}_{1,K} \\ \boldsymbol{O} & \cdots & \boldsymbol{O} & \boldsymbol{\Gamma}_{2,K} \\ \vdots & \ddots & \vdots & \vdots \\ \boldsymbol{O} & \cdots & \boldsymbol{O} & \boldsymbol{\Gamma}_{K,K} \end{pmatrix}.
$$

5 Numerical examples

In this section, we focus on video streaming which is one of the most important real-time applications, and evaluate the recovery performance of FEC using the analytical results derived in the previous section. It is assumed that the transmission rate of streaming data is 4 Mb/s, and that the video frame rate is 30 frame/s. The size of a packet is 500 bytes. A frame has $D = 34$ original data packets, and a block has the same number of packets as that of a frame. It is also assumed that the inter-arrival times of packets in main traffic are constant. We assume that the mean Good-state period is 19 times longer than the Bad-state one, i.e., $\beta/\alpha = 19$. When the output transmission rate of the wireless base station in Good state (resp. Bad state) is 40 Mb/s (resp. 4 Mb/s), the corresponding service rate of a 500 byte-packet μ_G (resp. μ_B) is 1.0×10^4 (resp. 1.0×10^3) [packet/s]. We define FEC redundancy as N/D. Note that when the sender host adds N redundant packets to D original data packets, the resulting packet transmission rate is $(D+N)/D$ times larger than the original one.

We validate the analytical model by simulation experiments driven by traces of the NLANR repository [19]. We conducted simulation experiments using the C program that we developed. The trace data was used for the inter-arrival times of background traffic, and the other settings are the same as the analysis. Table 1 shows the details of the trace data used for simulation experiments in the paper. Figure 2 illustrates the average volume of the trace data. As shown in Fig. 2, two subsets

Table 1
General information about the trace used for simulation experiments.

Name	Original filename	Date/Capt. on	Duration
Leipzig-II	20030221-121359-0.g2	February 2003/OC3	164 min.
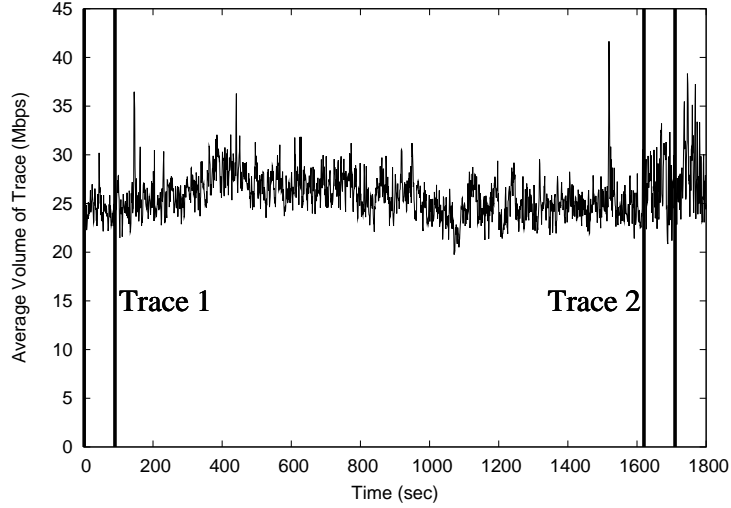
Fig. 2. Average volume of trace vs. time.
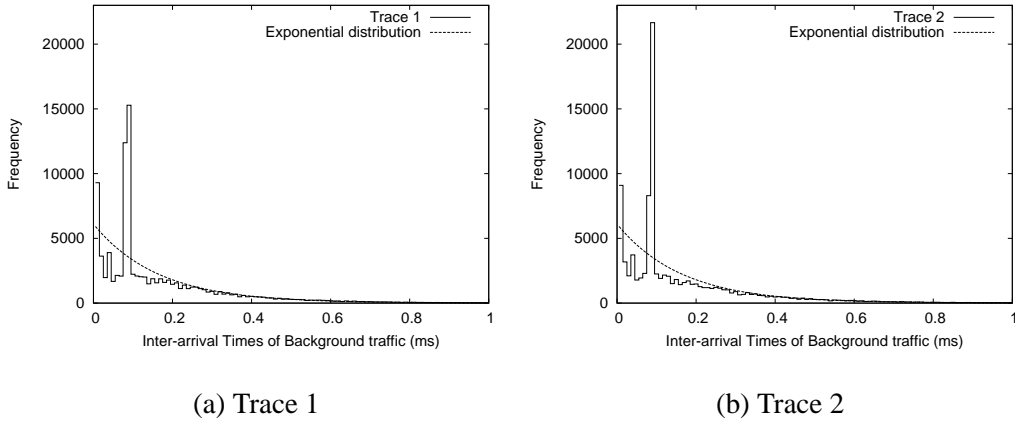
(a) Trace 1

(b) Trace 2

Fig. 3. Histogram of trace data and the corresponding exponential probability density function.

of the trace data were used for the simulation experiments. Trace 1 corresponds to the first 90 seconds of the original trace data. Trace 2 represents the 90 seconds of the trace data whose volume varies greatly. Each trace was used for the inter-arrival times of packets in background traffic.

Figure 3 illustrates the histogram of the trace data and the probability density function of the exponential distribution whose arrival rate is equal to that of the trace data. Fig. 3(a) (resp. 3(b)) shows the histogram of trace 1 (resp. trace 2). When the packet size is 500 bytes, the volume of trace 1 (resp. trace 2) is equal to 24.4 Mb/s (resp. 26.9 Mb/s) and the corresponding arrival rate λ is 6.10×10^3 (resp. 6.73×10^3) [packet/s]. The variance of the packet inter-arrival times for trace 1 (resp. trace 2) is 3.14×10^{-2} (resp. 2.78×10^{-2}), while that for the exponential distribution is 2.68×10^{-2} (resp. 2.21×10^{-2}), i.e., the variance of the traces is greater than that of the Poisson process.

11

Table 2
Basic parameters.

Parameter	Value
Number of original data packets in a block D	34
Number of redundant data packets in a block N	0, 1, 3
Ratio of β to α (β/α)	19
Service rate of a 500 byte-packet in Good state μ_G	1.0×10^4
Service rate of a 500 byte-packet in Bad state μ_B	1.0×10^3
Arrival rate of background traffic λ (Trace 1)	6.10×10^3
Arrival rate of background traffic λ (Trace 2)	6.73×10^3
System Size K	10, 100

5.1 *Impact of transmission rate in Good state*

In this subsection, we investigate how the transmission rate in Good state affects both the block- and packet-level loss probabilities. Figure 4 illustrates the block-loss probability against the transmission rate in Good state in cases of the system capacity $K = 10$ and 100. In each K, we calculated the block-loss probabilities for $N = 0, 1$ and 3. Analytical results are shown with lines, compared with simulation results represented by dots with 95% confidence intervals. Figure 4(a) (resp. 4(b)) shows the result of trace 1 (resp. trace 2), whose average volume of background traffic is 24.4 Mb/s (resp. 26.9 Mb/s). When the transmission rate in Good state is γ Mb/s, the corresponding packet service rate μ_G is equal to $\gamma \times 250$ [packet/s]. The transmission rate in Bad state is 4 Mb/s ($\mu_B = 1.0 \times 10^3$ [packet/s]), and the mean Bad-state period is 5 ms. Table 3 shows the difference between analysis and simulation in Figures 4(a) and 4(b) when the transmission rate in Good state is 50 Mb/s. In this table, "Difference" is calculated by subtracting "Analysis" from "Simulation".

First, we observe from Fig. 4 that the analytical results exhibit a good agreement with the simulation results for a large transmission rate in Good state. It is also observed from Fig. 4 and Table 3 that the simulation results of trace 1 agree better with analytical ones than those of trace 2. This is because the variance of volume of trace 2 is larger than that of trace 1. Furthermore, Fig. 4 shows that the block-loss probability decreases monotonically and then remains constant when the transmission rate in Good state is large. This is because a large transmission rate makes the traffic intensity small, resulting in a small block-loss probability. This result implies that the block-loss probability is not greatly affected by the transmission rate in Good state.
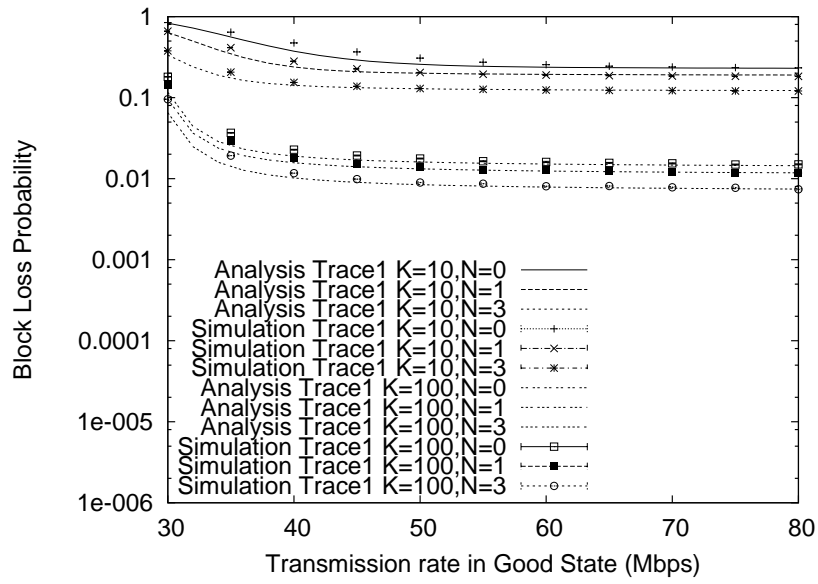
(a) Trace 1
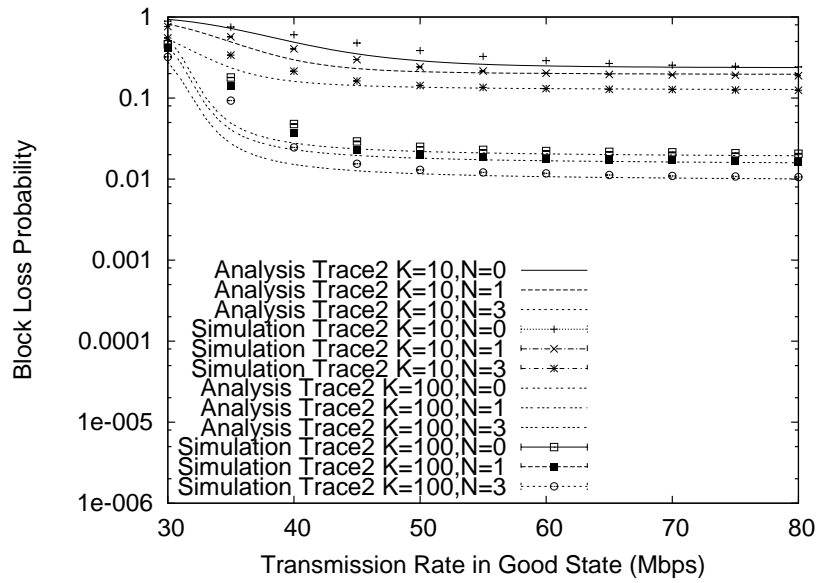
(b) Trace 2

Fig. 4. Block-loss probability vs. transmission rate in Good state.

In terms of FEC recovery performance, when the transmission rate in Good state increases, the block loss probability for $K = 100$ rapidly converges, while that for $K = 10$ decreases gradually. Because the traffic intensity in Bad state is larger than that in Good state, the burstiness of the loss process in Bad state is larger than that in Good state. This implies that FEC is not effective for the packet loss in Bad state. When the system capacity is small, the event of packet loss occurs not only in Bad
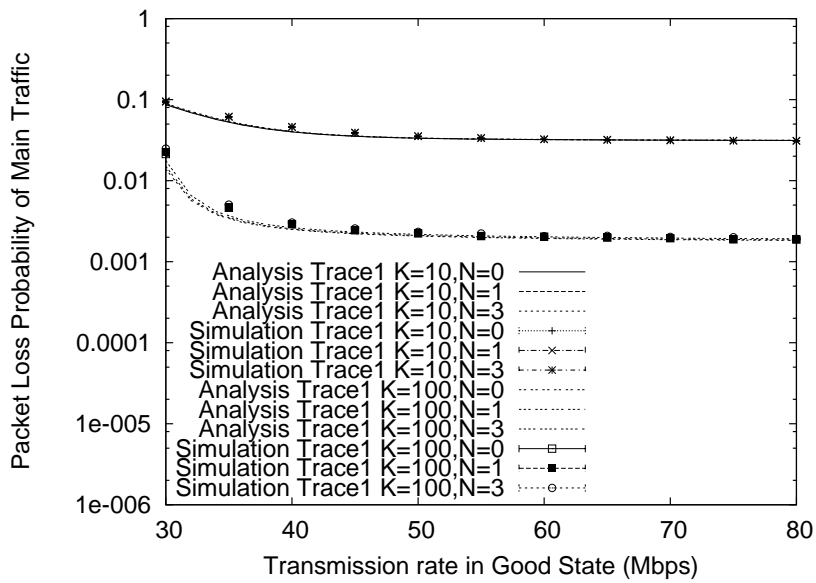
(a) Trace 1
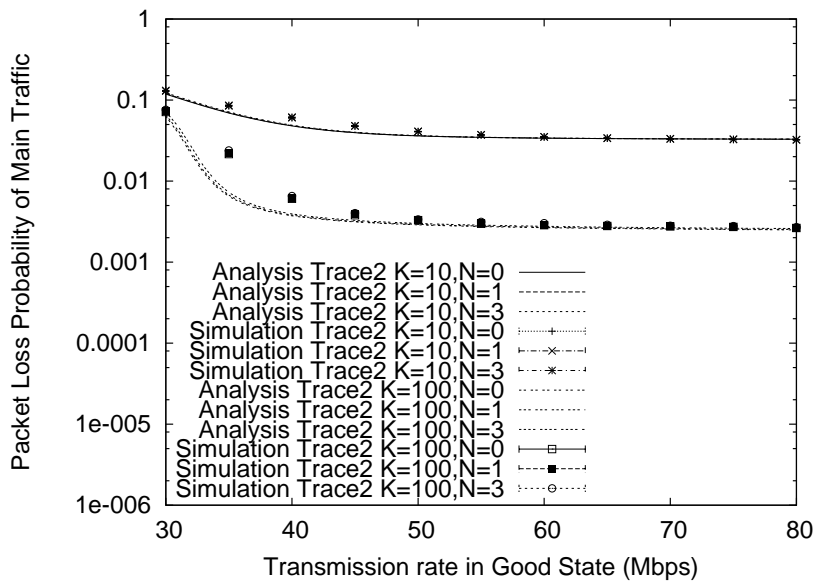
(b) Trace 2

Fig. 5. Packet-loss probability of main traffic vs. transmission rate in Good state.

state but also in Good state. When the transmission rate in Good state is large, the packet-loss probability in Good state decreases, resulting in high burstiness of loss process. This high burstiness degrades the recovery performance of FEC.

Figure 5 shows the packet-loss probability of main traffic against the transmission rate in Good state under the same condition as in Fig. 4. In Fig. 5, the packet

14

Table 3
Difference between analysis and simulation. (The transmission rate in Good state: 50 Mb/s)

K	N	Trace 1			Trace 2		
		Simulation	Analysis	Difference	Simulation	Analysis	Difference
10	0	0.307307	0.257376	0.049931	0.385827	0.288339	0.097488
10	1	0.204144	0.199948	0.004196	0.242284	0.211788	0.030496
10	3	0.129754	0.128596	0.001158	0.142798	0.136060	0.006738
100	0	0.017704	0.016059	0.001645	0.025046	0.021932	0.003114
100	1	0.013960	0.013221	0.000739	0.019711	0.018113	0.001598
100	3	0.008953	0.008434	0.000519	0.012988	0.011624	0.001364

loss probability of main traffic for both $K = 10$ and 100 decreases monotonically and then remains constant when the transmission rate in Good state is large. Note that the packet loss is likely to occur only in Bad state when the transmission rate in Good state is large. As a result, the transmission rate in Good state has small effect on the packet-loss probability. In Fig. 5, the packet-loss probability of main traffic is large when the number of redundant packets increases. This is simply because adding redundant packets enlarges the traffic intensity. Note here that the packet-loss probability of main traffic is not greatly affected by the increase in FEC redundant packets. The above results imply that the packet-loss process of main traffic is not greatly affected by the transmission rate in Good state.

Note that in Figs. 4 and 5, the analysis underestimates both the block- and packet-loss probabilities in comparison with simulation. In particular, the discrepancy between analysis and simulation is large for a small transmission rate in Good state. This is mainly because the packet interarrival times of the trace data, which are used for background traffic, are more correlated than the Poisson process assumed for the analytical model. It is well known that a Poisson input process gives an optimistic estimate of performance measures such as the packet loss probability and delay [18]. Though the analysis gives underestimated values of block- and packet-loss probabilities, a remarkable point here is that the analytical results are almost the same as the simulation results when the transmission rate in Good state is greater than 50 Mb/s. This implies that the analysis can be applied to a wired-wireless network whose wireless part is supported by IEEE 802.11a/g.

5.2 Impact of transmission rate in Bad state

In this subsection, we investigate how the transmission rate in Bad state affects the block-loss probability. Figure 6 shows the block-loss probability against the transmission rate in Bad state in cases of $K = 10, 100$ and $N = 0, 1, 3$. The Figure 6(a) (resp. 6(b)) shows the case of trace 1 (resp. trace 2), whose average volume of
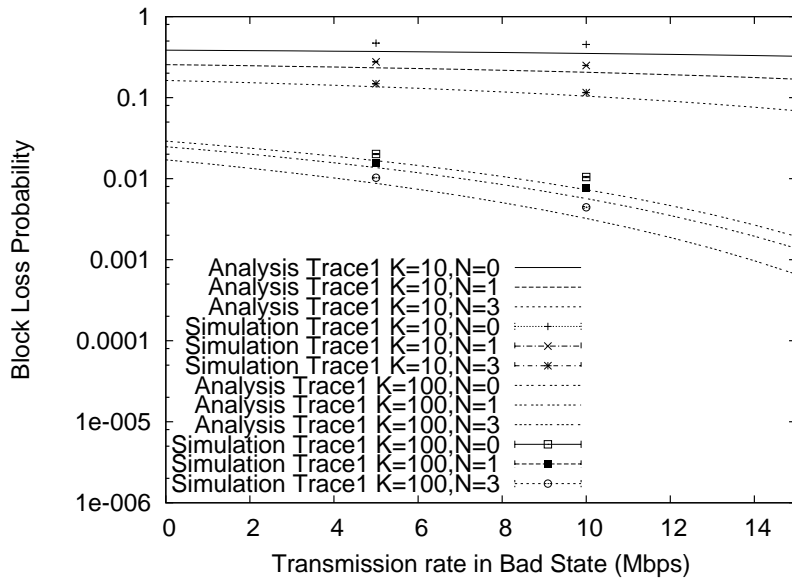
(a) Trace 1
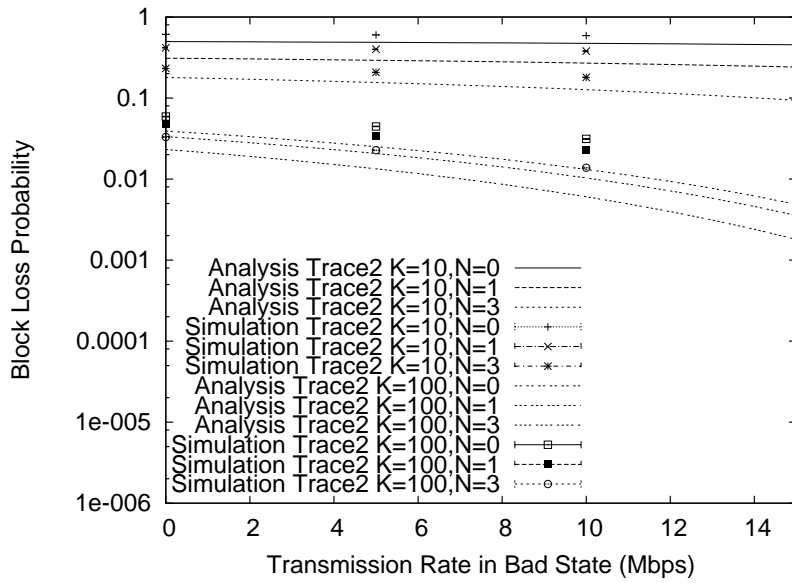
(b) Trace 2

Fig. 6. Block-loss probability vs. transmission rate in Bad state.

background traffic is 24.4 Mb/s (resp. 26.9 Mb/s). The transmission rate in Good state is 40 Mb/s ($\mu_G = 1.0 \times 10^4$ [packet/s]), and the mean Bad-state period is 5 ms.

It is observed from Fig. 6 that the simulation results of trace 1 agree well with analytical ones in comparison with those of trace 2, and that the block-loss probability

16

for trace 2 is larger than that for trace 1. This is because the average volume of trace 2 is larger than that of trace 1. Figure 6 shows that the analytical results agree well with the simulation ones for a small transmission rate in Bad state. The decrease in the transmission rate in Bad state makes the variance of the transmission time large. This large variance of the transmission time affects the queue length distribution, resulting in the decrease in the difference between the results of analysis and those of simulations. From Figs. 4 and 6, we observe that the block-loss probability by analysis is almost the same as that by simulation when the transmission rate of Good state greatly differs from that of Bad state.

Figure 6 shows that the block-loss probability for $K = 10$ is likely to remain constant when the transmission rate in Bad state is large. On the other hand, the block-loss probability for $K = 100$ decreases gradually against the transmission rate in Bad state. When the system capacity is large, a packet loss is likely to occur in Bad state. This implies that the block-loss probability is greatly affected by the transmission rate in Bad state. On the other hand, when the system capacity is small, a packet loss occurs in either Good state or Bad state. As a result, the effect of the transmission rate in Bad state on the block-loss probability is small. These results imply that the block-loss probability is affected by the system capacity and the transmission rate in Bad state.

In terms of FEC recovery performance, Fig. 6 shows that the block-loss probability for $K = 10$ is more improved by FEC than that for $K = 100$. In addition, the block-loss probabilities for both K's are not greatly improved by FEC when the transmission rate in Bad state is small. This is because a burst loss of packets is likely to occur in Bad state with a small transmission rate. This result implies that the recovery performance of FEC is limited for the wireless base station where the transmission rate of a packet greatly varies.

5.3   Impact of volume of background traffic

In this subsection, we investigate how the volume of background traffic affects the block-loss probability. Figure 7 illustrates the block-loss probability against the volume of background traffic in cases of $K = 10$ and 100. In each K, we calculated the block-loss probabilities for $N = 0, 1$ and 3. When the volume of background traffic is η Mb/s, the corresponding packet arrival rate λ is equal to $\eta \times 250$ [packet/s]. The transmission rate in Good state (resp. Bad state) is 40 Mb/s (resp. 4 Mb/s), and the mean Bad-state period is 5 ms. Note that Figure 7 shows only analytical results because the volume of the trace data used for simulation experiments is limited to 24.4 Mb/s and 26.9 Mb/s.

It is observed from Fig. 7 that the block-loss probability increases monotonically when the volume of background traffic is large. This is because a large volume of
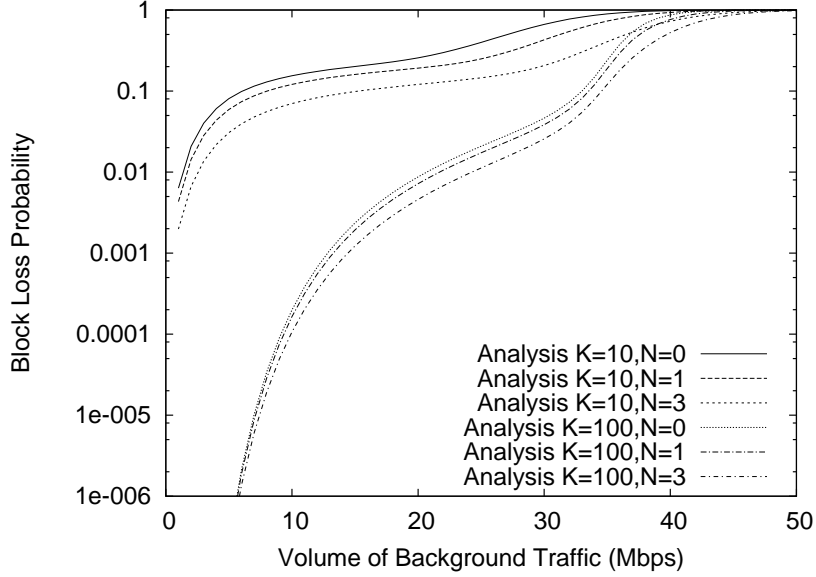
Fig. 7. Block-loss probability vs. volume of background traffic.

background traffic makes the traffic intensity large, resulting in a large block-loss probability. In case of $K = 100$, the block-loss probability exhibits rapid increases when the volume of background traffic is 5 Mb/s and 35 Mb/s. On the other hand, the block-loss probability increases gradually when the volume is around 20 Mb/s. Because the transmission rate in Bad state is much smaller than that in Good state, a packet loss is likely to occur in Bad state rather than in Good state. When the volume of background traffic increases, packet losses frequently occur even in Good state. In Fig. 7, this emerges at around 35 Mb/s in background traffic.

5.4 Impact of Bad-state period

In this subsection, we investigate how the mean Bad-state period affects the block-loss probability. Remind that the mean Good-state period is 19 times longer than the Bad-state one, i.e., $\beta/\alpha = 19$. Figure 8 shows the block-loss probability against the mean Bad-state period in cases of $K = 10$ and 100. In each K, we calculated the block-loss probabilities for $N = 0, 1$ and 3. The volume of background traffic is 24.4 Mb/s. The transmission rate in Good state (resp. Bad state) is 40 Mb/s (resp. 4 Mb/s).

It is observed from Fig. 8 that the analytical results agree well with the simulation ones for a long Bad-state period. In Fig. 8, we observe that the block-loss probability for $K = 100$ increases rapidly against the mean Bad-state period. On the other hand, the block-loss probability for $K = 10$ decreases gradually. When the system capacity is large, a packet loss is likely to occur only in Bad state. Therefore, when the Bad-state period is long, the packet-loss probability (and hence the block-loss probability) increases monotonically. When the system capacity is small, on the

18
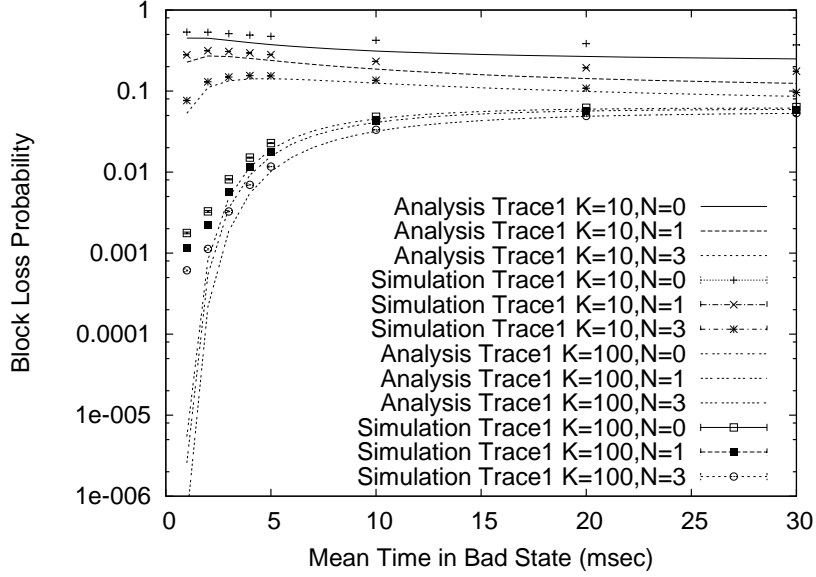
Fig. 8. Block-loss probability vs. mean time in Bad state.

other hand, the packet loss process depends on not only the Bad-state period but also the Good-state one. Noting that the ratio of the mean Good-state period to the Bad-state one is constant, the increase in the Bad-state period makes the Good-state period long. A longer duration staying in Good state causes less packet losses, resulting in a monotonic decrease in the block-loss probability for $K = 10$. The above results imply that the block-loss probability is greatly affected by the system capacity and the mean Bad-state period.

Note in Fig. 8 that each block-loss probability converges when the mean Bad-state period is sufficiently long in both $K = 10$ and 100. Because the mean Good-state period is 19 times longer than the Bad-state one, the queue length of the system in Good state is likely to be small when the mean Bad-state period is long. Therefore, a packet loss is likely to occur only in Bad state, making the block-loss probability close to the ratio of the mean Bad-state period to the mean cycle consisting of a Good-state period and a Bad-state period. In fact, we observe from Fig. 8 that the block loss probability approaches the value of $\alpha/(\alpha + \beta) = 0.05$.

Figure 9 shows the minimum FEC redundancy against the mean Bad-state period. The minimum FEC redundancy is defined as the minimum redundancy in units of packets to keep the block loss probability smaller than a prespecified value p. The minimum FEC redundancy was calculated for $p = 10^{-2}$, 10^{-3} and 10^{-4}. We observe from Fig. 9 that the minimum FEC redundancy for $K = 100$ is smaller than that for $K = 10$. This is because the packet-loss probability with a large buffer is smaller than that with a small one. It is also observed from Fig. 9 that the minimum FEC redundancy increases rapidly when the mean Bad-state period is long. When the Bad-state period is long, a burst loss of packets is likely to occur in Bad state. This high burstiness degrades the recovery performance of FEC, resulting in a large
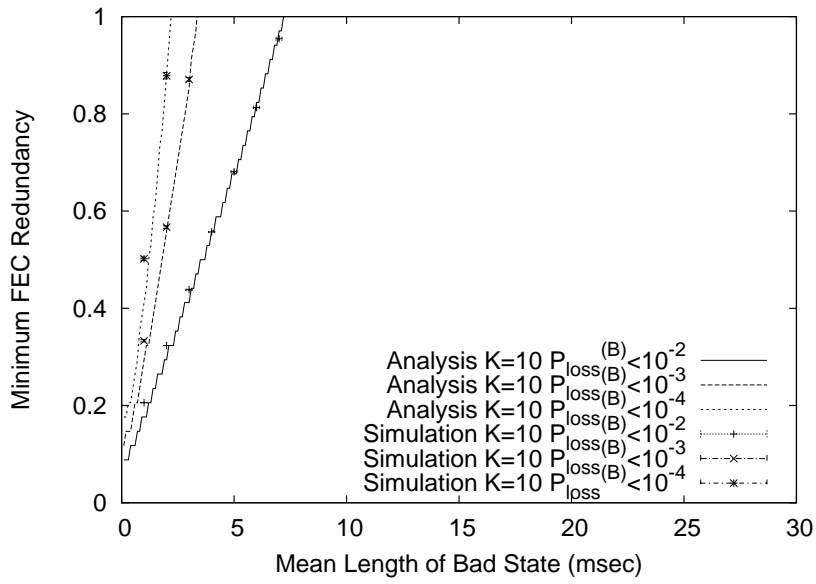
(a) $K = 10$
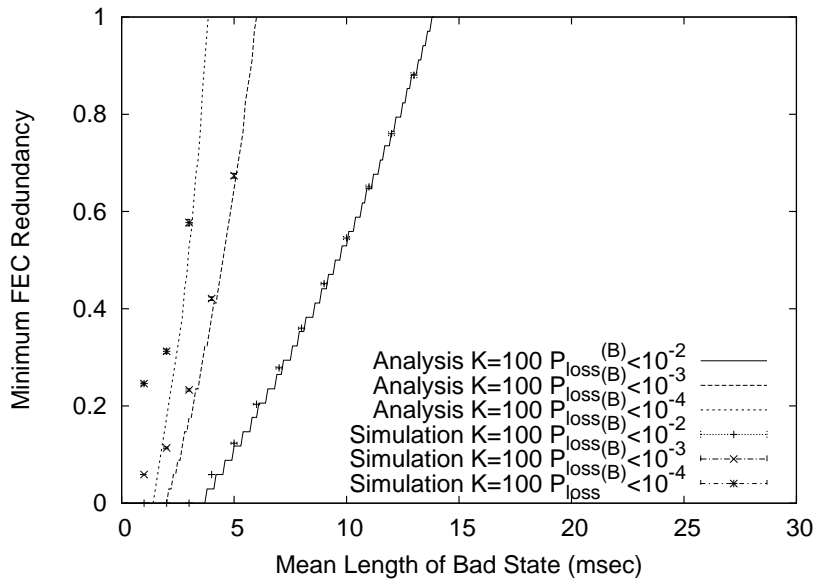
(b) $K = 100$

Fig. 9. Block-loss probability vs. ratio of Good-state period to Bad-state period.

minimum FEC redundancy.

Figure 10 represents the block-loss probability against β/α, the ratio of Good-state period to Bad-state one, in cases of $K = 10$ and 100. We set $1/\alpha = 50$ ms, and $1/\beta$ varies from 1 ms to 10 ms. Note that β/α lies in the range 10 to 50. In each K, we calculated the block-loss probabilities for $N = 0, 1$ and 3. The volume of
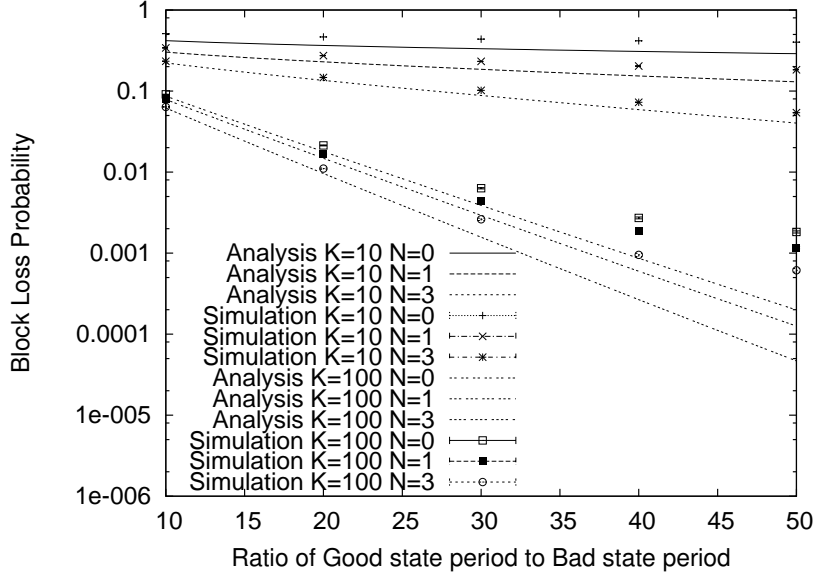
Fig. 10. Block-loss probability vs. ratio of Good-state period to Bad-state period.

background traffic is 24.4 Mb/s, and the transmission rate in Good state (resp. Bad state) is 40 Mb/s (resp. 4 Mb/s).

In Fig. 10, the block-loss probability becomes small with the increase in β/α for each set of K and N, as expected. In terms of the FEC redundancy, the block-loss probability also decreases with the increase in N. A remarkable point here is that the block-loss probability for $K = 100$ is significantly decreasing against β/α in comparison with that for $K = 10$. Note that the increase in β/α implies the improvement of the wireless link condition. Therefore, this result suggests that the block-loss probability for the system with a large buffer significantly decreases as the quality of the wireless link is improved.

Figure 11 shows the the minimum FEC redundancy against β/α. The minimum FEC redundancy was calculated for $p = 10^{-2}$, 10^{-3} and 10^{-4}. The other parameter values are the same as those in Fig. 10. Figure 11(a) represents the case for $K = 10$, while the block-loss probabilities for $K = 100$ are shown in Fig. 11(b). It is observed from both the figures that the minimum FEC redundancy is decreasing when β/α is large. We also observe that the minimum FEC redundancy for $K = 100$ is greatly smaller than that for $K = 10$. This also implies the effectiveness of a large buffer for improving the block-loss probability.

5.5 Impact of system capacity

Finally, we investigate how the system capacity affects the block-loss probability. We calculated the block-loss probabilities for $N = 0, 1$ and 3. The transmission rate in Good state (resp. Bad state) is 40 Mb/s (resp. 4 Mb/s), and the mean Bad-state
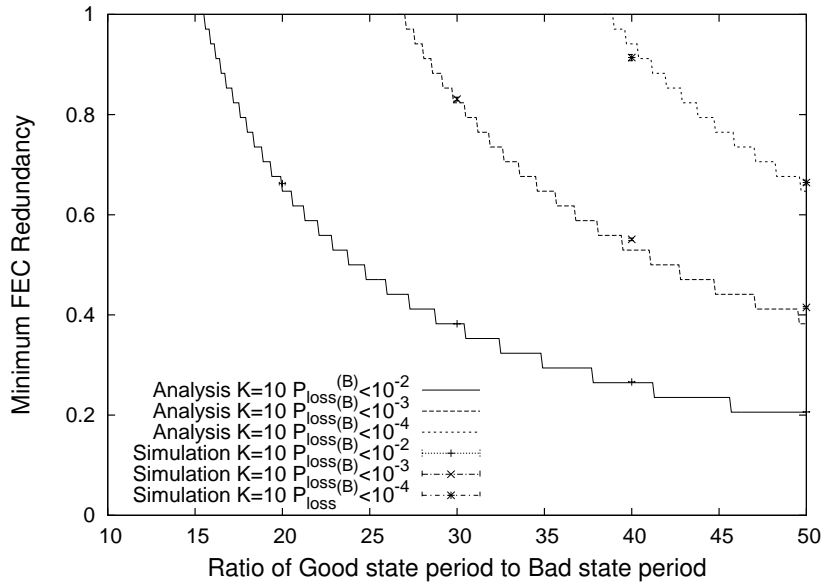
(a) $K = 10$
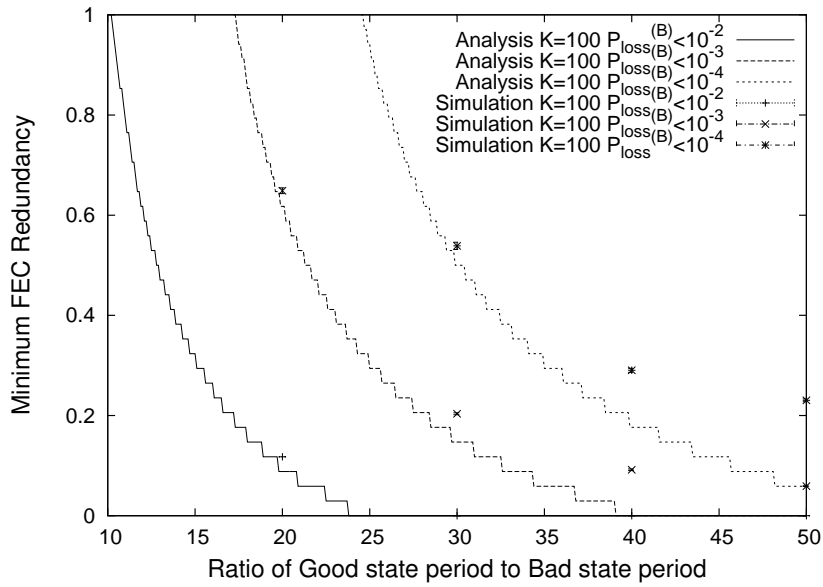
(b) $K = 100$

Fig. 11. Block-loss probability vs. ratio of Good-state period to Bad-state period.

period is 5 ms. The volume of background traffic is 24.4 Mb/s.

It is observed from Fig. 12 that the block-loss probability decreases at a constant rate when the system capacity is large. This implies that the block-loss probability is greatly affected by the system capacity. We also observe from Fig. 12 that the decay rate of the block-loss probability for each N is constant. This result suggests
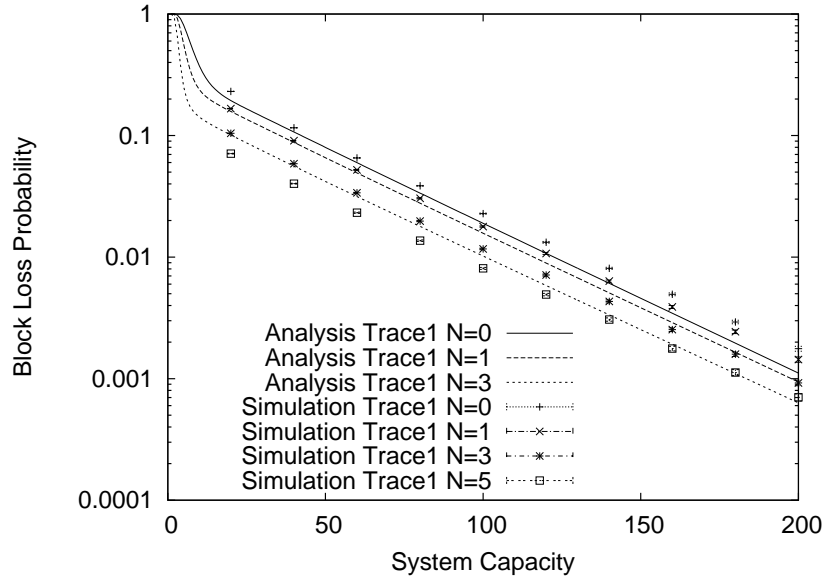
Fig. 12. Block-loss probability vs. system capacity.
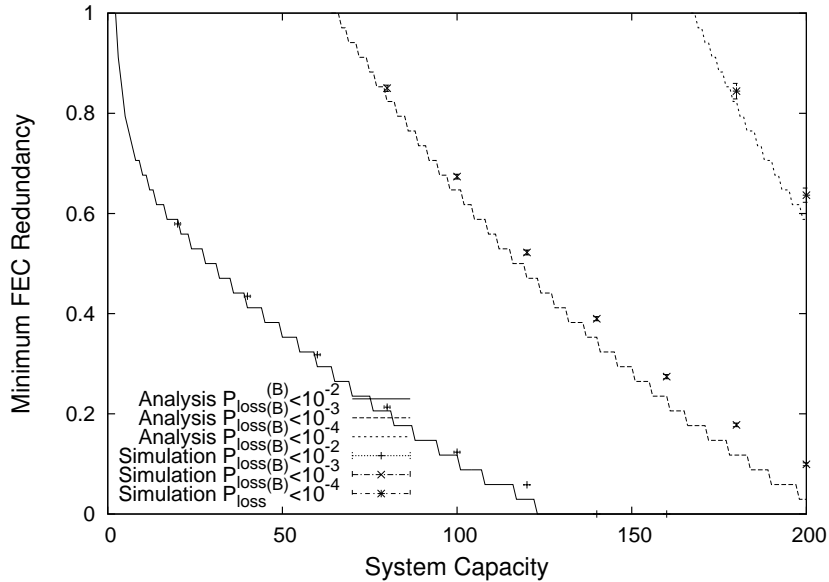
Fig. 13. Minimum FEC redundancy vs. system capacity.

that the block-loss probability is greatly improved by the system size, rather than FEC. Noting that a large buffer of the wireless base station makes the packet delay long when the packet-transmission scheduling is FIFO.

Figure 13 illustrates the minimum FEC redundancy against the system capacity. In Fig. 13, the minimum FEC redundancy decreases gradually when the system capacity is large. This result implies that the minimum FEC redundancy is dominated by the buffer size of the wireless base station. In other words, the FEC redundancy should be carefully determined by taking into consideration the buffer size of the wireless base station.

6 Conclusions

In this paper, we considered the recovery performance of FEC for video streaming services over wired-wireless networks. We modeled a wireless base station as a GI+M/MSP/1/K queue. The packet- and block-level loss probabilities were analyzed through a continuous-time Markov chain. It was shown from numerical examples that the block-loss probability is greatly affected by the system capacity and the mean Bad-state period. It was observed that the recovery performance of FEC deteriorates according to the fluctuation in the packet transmission rate at the wireless base station. It was also found that the block-loss probability is greatly improved by the system size, rather than FEC. When the packet scheduling of the buffer is FIFO, however, a large buffer causes a long packet delay. In video streaming services, a long packet delay also degrades the user-perceived video quality. Therefore, an appropriate packet scheduling should be adopted for a large-buffered wireless base station in order to support delay-sensitive application.

References

[1] I. F. Akyildiz, X. Wang and W. Wang, "Wireless Mesh Networks: A Survey," *Computer Networks,* vol. 47, no. 4, pp. 445-487, 2005.

[2] E. Altman and A. Jean-Marie, "Loss Probabilities for Messages with Redundant Packets Feeding a Finite Buffer," *IEEE Journal on Selected Areas in Communications,* vol. 16, no. 5, pp. 778-787, 1998.

[3] G. Carle and E. W. Biersack, "Survey on Error Recovery Techniques for IP-Based Audio-Visual Multicast Applications," *IEEE Network Magazine,* vol. 11, no. 6, pp. 24-36, 1997.

[4] N. M. Chaskar, T. V. Lakshman and U. Madhow, "TCP over Wireless with Link Level Error Control: Analysis and Design Methodology," *IEEE/ACM Transactions on Networking,* vol. 7, no. 5, pp. 605-615, 1999.

[5] I. Cidon, A. Khamisy and M. Sidi, "Analysis of Packet Loss Processes in High-Speed Networks," *IEEE Transactions on Information Theory,* vol. 39, no. 1, pp. 98-108, 1993.

[6] C. Cramer and E. Gelenbe, "Video Quality and Traffic QoS in Learning-Based Subsampled and Receiver-Interpolated Video Sequences," *IEEE Journal on Selected Areas in Communications*, vol. 18, no. 2, pp. 150–167, February 2000.

[7] C. Cramer, E. Gelenbe and H. Bakircioglu, "Low Bit Rate Video Compression with Neural Networks and Temporal Subsampling," *Proceedings of the IEEE*, vol. 84, no. 10, pp. 1529–1543, October 1996.

[8] G. Dán, V. Fodor and G. Karlsson, "On the Effects of the Packet Size Distribution on the Packet Loss Process," *Telecommunication Systems*, vol. 32, no. 1, pp. 31-53, 2006.

[9] G. Dán, V. Fodor and G. Karlsson, "On the Effects of the Packet Size Distribution on FEC Performance," *Computer Networks*, vol. 50, no. 6, pp. 1104-1129, 2006.

[10] Y. Feng and E. Gelenbe, "Adaptive object tracking and video compression," *Network and Information Systems Journal*, vol. 1, nos. 4–5, pp. 371–400, 1999.

[11] E. Gelenbe, C. Cramer, M. Sungur and P. Gelenbe, "Traffic and Video Quality in Adaptive Neural Compression," *Multimedia Systems*, vol. 4, pp. 357–369, 1996.

[12] P. E. Green, "Fiber to the Home: The Next Big Broadband Thing," *IEEE Communications Magazine,* vol. 42, no. 9, pp. 100-106, 2004.

[13] O. A. Hellal, E. Altman, A. Jean-Marie and I. A. Kurkova, "On Loss Probabilities in Presence of Redundant Packets and Several Traffic Sources," *Performance Evaluation,* vols. 36-37, nos. 1-4, pp. 486-518, 1999.

[14] K. Kawahara, K. Kumazoe, T. Takine and Y. Oie, "Forward Error Correction in ATM Networks: An Analysis of Cell Loss Distribution in a Block," in *Proc. IEEE INFOCOM'94,* pp. 1150-1159, 1994.

[15] S. Muraoka, H. Masuyama, S. Kasahara and Y. Takahashi, "Performance Analysis of FEC Recovery Using Finite-Buffer Queueing System with General Renewal and Poisson Inputs," *Managing Traffic Performance in Converged Networks (Proceedings of the 20th International Teletraffic Congress - ITC20)*, LNCS4516, Springer-Verlag, pp. 707-718, 2007.

[16] C. Perkins, O. Hodson and V. Hardman, "A Survey of Packet Loss Recovery Techniques for Streaming Audio," *IEEE Network Magazine,* vol. 12, no. 5, pp. 40-48, 1998.

[17] N. Shacham and P. Pckenney, "Packet Recovery in High-Speed Networks Using Coding and Buffer Management," in *Proc. IEEE INFOCOM*, vol. 1, pp. 124-131, 1990.

[18] V. Srinivasan, A. Ghanwani, E. Gelenbe, "Block Cell Loss Reduction in ATM Systems," *Computer Communications*, vol. 19, pp. 1077–1091, 1996.

[19] Passive Measurement and Analysis (PMA).
Available from:http://pma.nlanr.net/Special/leip2.html